

## Enhanced Swelling and Barrier Properties Stability of SPEEK-based Polymer Electrolytes Nanocomposite Membrane

J. Jaafar<sup>1</sup>, A. F. Ismail<sup>2\*</sup> & T. Matsuura<sup>3</sup>

<sup>1-3</sup>Advanced Membrane Technology Research Centre (AMTEC), Universiti Teknologi Malaysia, 81310 Johor Bahru, Johor, Malaysia

<sup>4</sup>Industrial Membrane Research Laboratory, Department of Chemical Engineering, University of Ottawa, 161 Louis Pasteur St., Ottawa, ON, KIN 6N5, Canada

### ABSTRACT

The objective of this study is to prepare SPEEK/Cloisite15A<sup>®</sup>/TAP nanocomposite membranes and to characterize their physicochemical properties as polymeric electrolyte nanocomposites. SPEEK membranes with various degrees of sulfonation (DS) were first prepared. Subsequently, 1 wt. % of Cloisite15A<sup>®</sup> and 2,4, 6-triaminopyrimidine (TAP), respectively, were introduced into the SPEEK matrices via solution intercalation method. The Cloisite15A<sup>®</sup> and TAP additives were used as reinforcing material for the SPEEK/Cloisite15A<sup>®</sup>/TAP (SP/CL/TAP) nanocomposite membranes in terms of the barrier properties, swelling and morphological structure. The effect of DS on the SP/CL/TAP nanocomposite membranes was studied in terms of their swelling behavior, proton conductivity and methanol permeability. Field emission scanning electron micrographs (FESEM) and X-Ray diffraction (XRD) patterns confirmed that the Cloisite15A<sup>®</sup> particles were completely distributed to allow the nanosize dispersion in the polymer matrix. The swelling behavior of SPEEK membrane at DS of 88% was improved in the presence of Cloisite15A<sup>®</sup> and TAP. All SPEEK nanocomposite membranes studied exhibited improved methanol barrier properties compared with the parent SPEEK membranes. Owing to significant conductivity, remarkable barrier properties, high swelling stability and outperformed DMFC performance, SP63/CL/TAP nanocomposite membranes can be considered as a polymer electrolyte membrane for DMFC applications.

*Keywords:*

### 1.0 INTRODUCTION

Over the last decade, polymer-inorganic composite ionic membranes have gained tremendous attention for the application in direct methanol fuel cell (DMFC). The addition of a functional inorganic, which includes the inorganic filler with the presence of functional groups such as sulfonics, phosphonic acids, and quarternary ammonium salts and etc., or nonfunctional

inorganic, i.e., weak ionic groups, for instance, carboxylic acids, hydroxyls, and primary, secondary and tertiary amine groups, into the organic material is usually practiced in proton exchange membranes (PEMs) to improve their mechanical and thermal stability, and performance. For decades, in the development process, perfluorosulfonated membranes and their composites with inorganic materials have been dominated and exhibited better thermal, mechanical stability and proton conductivities for DMFC. Concurrently, composite of hydrocarbon

\* Corresponding to: A. F. Ismail (email: afauzi@utm.my)

polymers, such as poly (ether ether ketone), poly (benzimidazole), poly (sulfone), poly (vinyl alcohol) etc., have been developed as alternatives to the high cost perfluorinated membranes [1-3].

The transport of proton in the PEMs is greatly affected by the presence of water molecules. Water molecules provide a probe of the local environment and hydrogen bond network dynamics of water confined in the hydrophilic region of cation exchange membrane materials. Therefore, water provides a better medium for protons to extremely mobile than in common ions environment. This is the result of the fact that proton in water does not take place through normal diffusion, but via a process where hydrogen bonds between water molecules are converted into covalent bonds, and vice versa [4]. Simultaneously, the transport of methanol through PEMs was also driven by the water molecules. However, this phenomenon will contribute to methanol crossover in which not favorable for DMFC application. Therefore, the development of new membranes which can conduct protons with little or no water and prevent methanol permeability would be the greatest challenge in the fuel cell community.

One of the promising strategies to improve PEMs performance is through improving the water management by incorporation of nanometer sized particles such as silica, titania and zirconia, which significantly can act as a water reservoir. Silica family attracted much attention in the development of polymer-inorganic membranes owing to its physical and chemical stability [5]. The addition of highly crystalline silica does not contributed to the formation of a uniform polymer solution because of its chemical or physical interaction is limited to the external surface (active surface). Therefore, the selection of amorphous silica clay is more favorable [6]. The modification of well ordered silica materials such as montmorillonite (MMT) into more amorphous clay, for instance the Cloisite clays, is crucial in order to improve the processability and performance of the polymer-inorganic materials. Cloisite15A<sup>®</sup> possesses the largest basal spacing (d spacing), i.e., 31.5Å as compared to the other commercial Cloisite clays available in the market. Therefore, Cloisite 15A<sup>®</sup> is more flexible, thus

can be fabricated according to the application commonly used in modifying the properties of the ionic polymers [7].

The commercially available silica nanoparticles i.e., nanosilica powder is mainly produced by the fuming and precipitation method in the industrial application. Fumed silica is a fine, white, odorless, and tasteless amorphous powder. In addition, fumed silica has an extremely large surface area with smooth nonporous surface, which could promote strong physical contact between the filler and the polymer matrix. Precipitated silica is a fine hydrated silica particle. In these two nanosilica materials, the precipitated silica is rarely used due to the presence of more silanol (Si-OH) groups on the surface and consequently it is much easier to agglomerate than fumed silica. The presence of the hydroxyl groups on the surface holds individual silica particles together and formed aggregate which in turn remain intact even under the best mixing condition during dope formulation [8]. With respect to Cloisite 15A<sup>®</sup>, it can be seen from Figure 1 that there is no hydroxyl groups presence in the chemical structure of Cloisite 15A<sup>®</sup> bound to the organic modifier [9]. Therefore, Cloisite 15A<sup>®</sup> is supposed to belong to the fumed silica category. However, some researchers reported that Cloisite 15A<sup>®</sup> particles were not well dispersed in the hydrocarbon polymer matrix [10]. This might be due to the presence of some Si-OH groups in the MMT clay structure, because it is assumed that the amount of Si-OH present in the MMT structure remains unchanged even after the attachment of the surfactant.

Addition of a compatibilizer such as 2,4, 6-triaminopyrimidine (TAP) into the dope, instead of just Cloisite15A<sup>®</sup>, is promising to enhance the compatibility between SPEEK and Cloisite15A<sup>®</sup> particle thus increasing the degree of dispersion of Cloisite15A<sup>®</sup> particles. Based on our best knowledge, these aspects were rarely studied. Therefore, the objective of this work is to study the effect of different degrees of substitution (DS) of SPEEK on the morphological structures, swelling behaviors and performance for DMFC application for the membranes fabricated from the mixtures of Cloisite15A<sup>®</sup>, TAP and the SPEEKs.

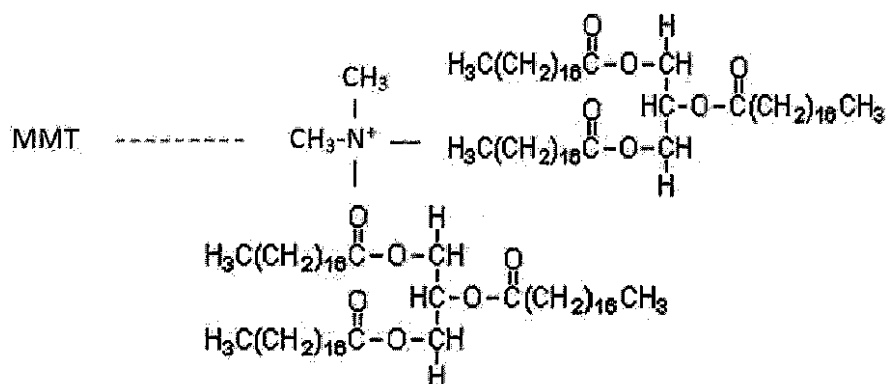


**Figure 1** Model of chemical structure of MMT with organic modifier (surfactant) formed Cloisite 15A<sup>®</sup>. The general composition of MMT is  $M^{+}_x(\text{Si}_{4-y}\text{Al}_y)[(\text{Al}, \text{Fe}^{3+})_{2-z}(\text{Mg}, \text{Fe}^{2+})_z]\text{O}_{10}(\text{OH})_2$ , where  $x=0.2-0.6$ ,  $x=y+z$ , and  $y < z$

## 2.0 EXPERIMENTAL

### 2.1 Materials

Poly (ether ether ketone) (PEEK) was obtained from Vitrex Inc., USA. Concentrated sulfuric acid (95-97%) purchased from QREX was used as the sulfonating agent for sulfonation process. Cloisite15A<sup>®</sup> was obtained from Southern Clay Products, Inc. and was used as received. The typical dry particle sizes of Cloisite15A<sup>®</sup> is 10% less than 2  $\mu\text{m}$ , 50% less than 6  $\mu\text{m}$  and 90% less than 13  $\mu\text{m}$ . Dimethylsulfoxide (DMSO) and 2,4,6-triaminopyrimidine (TAP) were obtained from Sigma-Aldrich and used as supplied as the solvent and as the compatibilizer, respectively.

### 2.2 Sulfonation Reaction Process

Sulfonation was carried out according to the method described elsewhere [11]. A mixture of 50 g PEEK and 1000 ml sulfuric acid was magnetically stirred at room temperature for 1 h. Then the solution was continuously stirred at 55°C, 60°C, 65°C and 70°C for 3 h in order to obtain different degrees of sulfonation (DS). The sulfonated polymer was recovered by precipitating the acid polymer solution into a large excess of ice-cube. The resulted SPEEK polymer was

filtered and washed thoroughly with deionized water until the pH (use pH paper) became 6 to 7. Finally, the sulfonated PEEK polymer was dried in the drying oven at 100°C for 24 h.

### 2.3 Preparation of Nanocomposite Membrane

10 wt. % of SPEEK solution was first prepared by dissolving SPEEK in DMSO. Desired amounts of Cloisite15A<sup>®</sup> (0.1 g) and TAP (0.1 g) were added to a small amount of DMSO in another container and the mixture was vigorously stirred for 24 h at room temperature. The latter mixture was then added to the SPEEK solution so that the total amount of DMSO becomes 90 mL. This mixture was formulated to produce the SPEEK membrane composited with 1.0 wt. % of Cloisite15A<sup>®</sup> and 1.0 wt. % of TAP. The SPEEK containing mixture was again vigorously stirred for 24 h at room temperature to produce a homogeneous solution. Before proceeding to the casting process, the mixture was heated to 100 °C to evaporate the DMSO solvent. This preparation method was known as solution intercalation method.

The polymer dope was then cast on a glass plate with a casting knife to form a solution film. The resultant film was then dried in a vacuum oven for 24 h at 80°C. The membrane was further dried for

6 h at 100°C to remove the residual solvent. After being detached from the glass plate, by immersing the membrane together with the glass plate into water, the membrane was dried for 3 days in a vacuum oven at 80°C. Finally, the membrane was treated with 1 M sulfuric acid solution for 1 day at room temperature and subsequently rinsed with water several times to remove the remaining acid.

## 2.4 Characterization Methods

### 2.4.1 Nuclear Magnetic Resonance Spectroscopy

Proton-nuclear magnetic resonance (<sup>1</sup>H-NMR) spectroscopy was used to determine the degree of sulfonation (DS) of parent SPEEK membranes. Based on the DS obtained, the ion exchange capacity (IEC) can be determined as well. <sup>1</sup>H-NMR spectra were recorded on a NMR spectrometer (Varian Unity Inova, Bruker, Switzerland) at a resonance frequency of 399.961 MHz at room temperature. For each analysis, 3 wt. % polymer solutions were prepared in deuterated dimethyl sulfoxide (DMSO-d<sub>6</sub>). The DS was determined by comparative integration of distinct aromatic signals. The ion exchange capacity (IEC) and DS of SPEEK in hydrogen form are related to each other by the following Equation [12].

$$DS\% = \frac{288(IEC)}{1000 - 80(IEC)} \times 100 \quad (1)$$

It should be mentioned that the equivalent weight of SPEEK in hydrogen form and PEEK are 368 and 288 respectively. The number (80) resulted from the difference between these two unit molecular weights [13].

Once the IEC of parent SPEEK was obtained from the <sup>1</sup>H-NMR analysis, the IEC of the SPEEK nanocomposite membranes can be estimated by the following Equation [13].

$$IEC_{\text{composite}} = \frac{[(IEC_{\text{SPEEK}} * m_{\text{SPEEK}}) + (IEC_{\text{additive1}} * m_{\text{additive1}}) + (IEC_{\text{additive2}} * m_{\text{additive2}})]}{m(\text{SPEEK} + \text{additives})} \quad (2)$$

where,  $m_{\text{SPEEK}}$  is the weight load of SPEEK and

$m_{\text{additive}}$  is the weight load of additives incorporated into the SPEEK formulation.

### 2.4.2 Morphological Characterization

For observation of the dispersion of Cloisite 15A<sup>®</sup> in the SPEEK/Cloisite 15A<sup>®</sup>/TAP membrane, the Field-Emission Scanning Electron Microscopy (FESEM) (JSM-6701F, JEOL USA, Inc.,) with resolution of 25,000 magnification was used.

### 2.4.3 X-ray Diffraction Analysis (XRD)

Nanocomposite formation and the degree of Cloisite 15A<sup>®</sup> dispersion were monitored using XRD (Philip PW1710 XRD, Netherlands) with nickel filtered Cu K $\alpha$  source ( $\lambda = 0.154056$  nm) at 30 kV and 30 mA. The diffractogram was scanned with a scanning rate of 2° min<sup>-1</sup> in a 2 $\theta$  range of 1.5–10° at room temperature. The d-spacing of Cloisite 15A<sup>®</sup> in nanocomposites was calculated using Bragg's equation based on XRD results:

$$d = \frac{n\lambda}{2 \sin \theta} \quad (3)$$

### 2.4.4 Swelling Behavior Measurement

Membrane samples with 2.5 cm of diameter were dried in an oven at 60°C for 48 h. The weighed or dimensions (thickness/diameter) measured films were then soaked in deionized water overnight at room temperature and at elevated temperature and then blotted dry with absorbent paper to remove any surface moisture, and then reweighed or measured the membranes' dimensions. Similar method was repeated for methanol solution swelling behavior with different methanol concentration and was carried out at room temperature. Later, the water/methanol uptake was calculated as follows,

$$\text{Water/methanol uptake} = \frac{W_{\text{wet}} - W_{\text{dry}}}{W_{\text{dry}}} \times 100 \quad (4)$$

where,  $W_{\text{wet}}$  is the weight of the wet membrane and  $W_{\text{dry}}$  the weight of the dry membrane.

The dimensional change ratio in plane and thickness was defined by Equation (5) and (6),

respectively. For the dimensional change ratio in plane, the length of the membrane was measured in different directions on the membrane surface and the resulting values were averaged. For the dimensional change ratio in thickness, the thickness of the wet tested membranes was measured by using the digital micrometer and three replicates data was taken and the results were presented as average data.

$$\text{Swelling in plane} = \frac{L_{\text{wet}} - L_{\text{dry}}}{L_{\text{dry}}} \times 100 \quad (5)$$

where,  $L_{\text{wet}}$  is the length (in diameter) of the wet membrane and  $L_{\text{dry}}$  the length of the dry membrane.

$$\text{Swelling in thickness} = \frac{d_{\text{wet}} - d_{\text{dry}}}{d_{\text{dry}}} \times 100 \quad (6)$$

where,  $d_{\text{wet}}$  is the length of the wet membrane and  $d_{\text{dry}}$  the length of the dry membrane.

#### 2.4.5 Proton Conductivity Measurement

The proton conductivity of the membrane was measured by AC impedance technique using a Solartron impedance-gain phase analyzer as detailed elsewhere [14]. All impedance measurements were performed at room temperature and 100% relative humidity (RH). The membrane resistance,  $R$ , was obtained from the intercept of the impedance curve with the real-axis at the high frequency end. Then, proton conductivity of membrane,  $\sigma$  ( $\text{Sm}^{-1}$ ), was calculated according to Equation (7).

$$\sigma = \frac{d}{RS} \quad (7)$$

where,  $d$  and  $S$  are the thickness of the hydrated membrane and the area of the membrane sample, respectively.

#### 2.4.6 Methanol Permeability Measurement

The methanol permeability of SPEEK and its nanocomposite membranes was measured as described in the previous work [14]. Equation (8) expresses the methanol permeability of the

membranes. The methanol permeability test was carried out for 3 h at room temperature. The methanol permeability,  $P$ , value was calculated using the following equation,

$$P = \alpha \times \frac{V_B}{A} \times \frac{L}{C_A} \quad (8)$$

where,  $P$  is methanol permeability,  $\alpha = \frac{C_B(t)}{(t-t_0)}$

the slope of linear interpolation of the plot of methanol concentration in the permeate compartment,  $C_B(t)$ , versus time,  $t$ ,  $V_B$  is the volume of the water compartment,  $A$  is the membrane cross-sectional area (effective area),  $L$  is thickness of the hydrated membrane and  $C_A$  is the concentration of methanol in the feed compartment,  $t_0$  is time lag, related to the diffusivity.

#### 2.5 DMFC Performance

The active surface area of the MEA was  $5.0 \text{ cm}^2$  and was composed of PtRu-supported carbon catalyst ( $1.0 \text{ mg/cm}^2$  as Pt amount) with binder of Nafion DE1021CS (Binder/ Carbon = 1) for cathode. PtRu-supported carbon catalyst ( $1.0 \text{ mg/cm}^2$  as Pt amount) with binder of Nafion DE1021CS (Binder/ Carbon = 0.75) was used in anode. MEAs from the tested membranes were prepared by hot pressing the membranes on the electrodes. After conducting the MEAs at different pressure, temperature and time consuming to adhere the PEM and electrodes, it was found that the at 3 Nm pressure and  $80^\circ\text{C}$  for 2 min could prevent leakage at the electrodes edge that contact with PEM.

The single DMFC performance was evaluated by recording the cell voltage vs. current density curves using a fuel cell analyzer test system (PRO200F, PRO-POWER communication Co. Ltd, USA). PROF200F is designed to allow current loading up to 20 A through fuel (fuel supply controlled by stepping motor) and air flow rate control (air supply controlled by automatic air controller). It provides Windows XP environment

**Table 1** Sulfonation reaction conditions of SPEEK and its nanocomposite membranes with various degree of sulfonation (DS)

Sample designation	Sulfonation reaction time (h)	Sulfonation reaction temperature (°C)	Degree of sulfonation (%)	Ion exchange capacity, IEC (m equiv./g) <sup>a</sup>
SP50	3	55	50	1.5244
SP63	3	60	63	1.8617
SP77	3	65	77	2.2025
Sp88	3	70	88	2.4554
SP50/CL/TAP	3	55	50	1.5068
SP63/CL/TAP	3	60	56	1.8375
SP77/CL/TAP	3	65	76	2.1716
SP88/CL/TAP	3	70	86	2.4195

<sup>a</sup> IEC values of parent SPEEK with various DSs were obtained from <sup>1</sup>H-NMR analyses, IEC values of SPEEK nanocomposites with various DSs were estimated from Equation (2)

with simple data storage and Excel conversion to facilitate understanding of test conditions and obtaining result values. Air rate (100 % relative humidity) with flow rate 100 ccmin<sup>-1</sup> and methanol (3 M) with flow rate 1 ccmin<sup>-1</sup>, were supplied to the cathode and anode, respectively. The gold coated electronic load terminal was designed to exactly measure load by minimizing electric resistance. This is therefore, the current load, temperature, air and fuel flow rate can vary automatically. The current loadings were varied from 50-300 mAcm<sup>-2</sup> for 20 min. The sequence current changes were repeated two times after cell temperature became 60°C. Once the temperature became 60°C, the DMFC performance measurement was conducted three times, and the results were presented as the average data.

### 3.0 RESULTS AND DISCUSSION

#### 3.1 SPEEK and SPEEK/Cloisite15A<sup>®</sup>/TAP Nanocomposite Membranes

SPEEK consists of highly hydrophilic charged sulfonic acid group and highly hydrophobic PEEK backbone, therefore SPEEK is differentiated into two environments, the hydrophilic environment (consisting of the polar SO<sub>3</sub>H groups) and the hydrophobic environment (consisting of the rest of the SPEEK matrix) [15]. In this work, the degree of sulfonation was controlled by varying the temperature while maintaining the reaction time. Table 1 summarizes the sulfonation conditions of SPEEK with different DSs.

Homogenous dispersion of nano-meter sized inorganic fillers into sulfonated polymers is known to generate nanocomposite membranes with improved morphological stability induced by hydrogen bonding, thus allowing to maintain conductive properties without excessive swelling [16]. In the present work nanocomposite membranes were fabricated from the solutions in

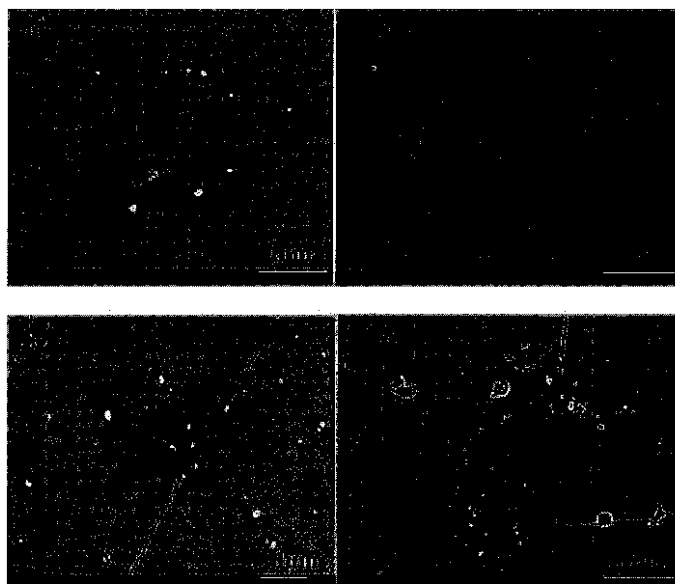


**Figure 2** FESEM surface images of SPEEK nanocomposite membranes (a) SP50/CL/TAP; (b) SP63/CL/TAP; (c) SP77/CL/TAP and (d) SP88/CL/TAP

which intercalated Cloisite15A<sup>®</sup> particles were dispersed into SPEEK matrix in the presence of TAP (compatibilizer). Thus, the prior contribution of this work was to fill the space between Cloisite15A<sup>®</sup> particles and the SPEEK matrix with the compatibilizer and to form disordered Cloisite15A<sup>®</sup> network.

The idea of incorporating Cloisite15A<sup>®</sup> into SPEEK with various degrees of sulfonation (DS) arose because it was realized that SPEEKs of high DSs tend to swell in water and methanol even at room temperature [17]. Incorporation of the Cloisite15A<sup>®</sup> and TAP in SPEEK is believed to enable the water content management by providing additional water reservoir without having excessive membrane swelling.

### 3.2 Degree of Sulfonation (DS) and Ion Exchange Capacity (IEC) Studies by using <sup>1</sup>H-NMR

<sup>1</sup>H-NMR analysis was performed to determine the DS and IEC of the SPEEK. Once the IEC value of the SPEEK with various DSs was obtained from the <sup>1</sup>H-NMR, the IEC of the SPEEK

nanocomposite membranes was estimated by using Equation (2).

Table 1 shows the IEC values of the parent SPEEK and the SPEEK nanocomposite membranes. It is clearly showed that the SPEEK nanocomposite membranes have lower IEC values than the parent SPEEK membranes with similar DS. This phenomenon is natural because in the presence of filler, the weight of the membrane is increased. Thus the concentration of sulfonic acid groups in the polymer chain was decreased per unit volume [18-19].

### 3.3 Morphological Structural Studies by Field Emission Scanning Electron Microscopy (FESEM)

Figure 2(a)-(d) show the FESEM images of SP50/CL/TAP, SP63/CL/TAP, SP77/CL/TAP and SP88/CL/TAP nanocomposite membranes, respectively. At this level of magnification, i.e., 25,000 $\times$ , there does not appear to be any serious agglomeration of Cloisite15A<sup>®</sup> particles in the SPEEK matrix for all samples, which suggests that the addition of TAP did indeed improve the

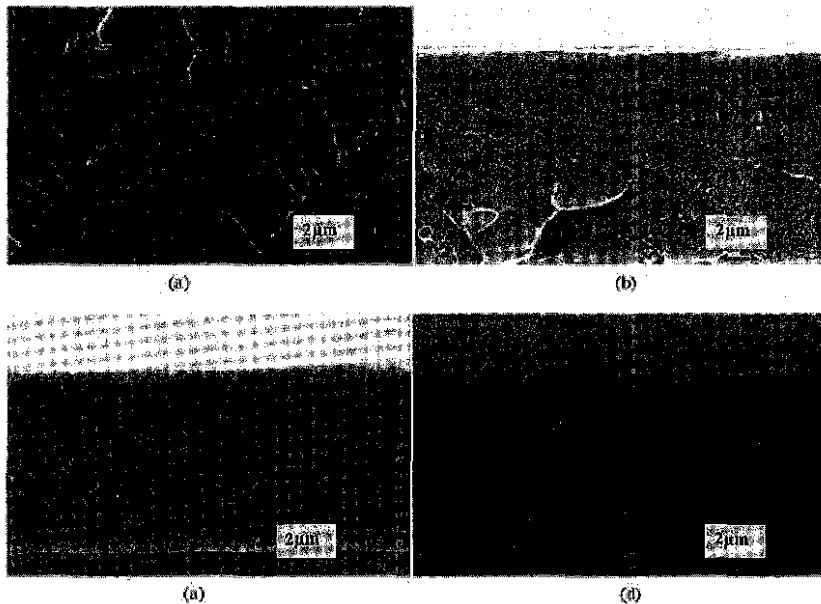


**Figure 3** FESEM cross-section images of SPEEK nanocomposite membranes (a) SP50/CL/TAP; (b) SP63/CL/TAP; (c) SP77/CL/TAP and (d) SP88/CL/TAP

compatibility between SPEEK and Cloisite15A<sup>®</sup>. However, Figure 2(c) and (d) show some fractures on the upper surface of SP77/CL/TAP and SP88/CL/TAP membrane images. This suggests that dispersion of Cloisite15A<sup>®</sup> particles in SP77/CL/TAP and SP88/CL/TAP were less uniform in the presence of a large amount of the sulfonate group. Probably, in the presence of an excessive amount of SO<sub>3</sub>H, most of the basic functional groups of TAP are bound to the SO<sub>3</sub>H group and not many are left to be bound to Cloisite15A<sup>®</sup>. Thus, TAP can no longer act as a bridge between Cloisite15A<sup>®</sup> and SPEEK, diminishing the TAP's function as a compatibilizer.

According to FESEM cross-section images of SP50/CL/TAP, SP63/CL/TAP, SP77/CL/TAP and SP88/CL/TAP nanocomposite membranes from Figure 3(a)-(d), similar observation as FESEM surface images of the nanocomposite membranes can be seen. It was hardly to notice any agglomeration of Cloisite15A<sup>®</sup> in the SP50/CL/TAP and SP63/CL/TAP cross-section images. This might be due to the low amount of Cloisite15A<sup>®</sup> loading in the nanocomposite membrane and the significant uniform dispersion

of Cloisite15A<sup>®</sup> throughout the SPEEK polymer matrix. Unfortunately, even at low amount of Cloisite15A<sup>®</sup> addition in the nanocomposite mixture, SP77/CL/TAP and SP88/CL/TAP still shows the appearance of Cloisite15A<sup>®</sup> particles aggregations. Moreover, the emergence of voids indicates the insignificant compatibility of Cloisite15A<sup>®</sup> at higher sulfonic acid attachment though in the presence of TAP.

### 3.4 Dispersion State of Cloisite15A<sup>®</sup> Study by X-Ray Diffraction (XRD)

The morphology of the Cloisite15A<sup>®</sup> particles and SPEEK/ Cloisite15A<sup>®</sup>/ TAP nanocomposite membrane with different DSs was also determined by using the XRD patterns, which are illustrated in Figure 4 and 5, respectively. Some researchers reported that there were two diffraction peaks, i.e.,  $2\theta \sim 7^\circ$  and  $19^\circ$  that reflected the planes (001) and (002), respectively, of the corresponding Cloisite15A<sup>®</sup> clay [20, 21]. However, in this study, the XRD patterns of the corresponding clay were only observed in a small angle part in the range of  $2^\circ$  to  $10^\circ$  of  $2\theta$  scale



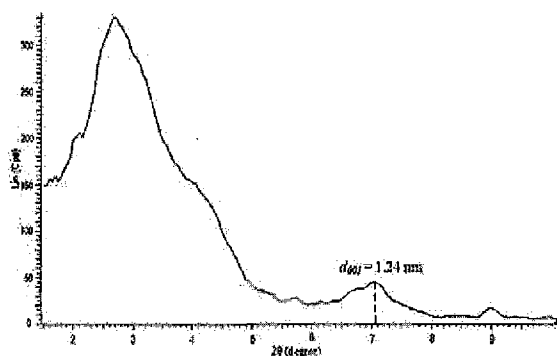


Figure 4 XRD patterns of pure Cloisite 15A<sup>®</sup>

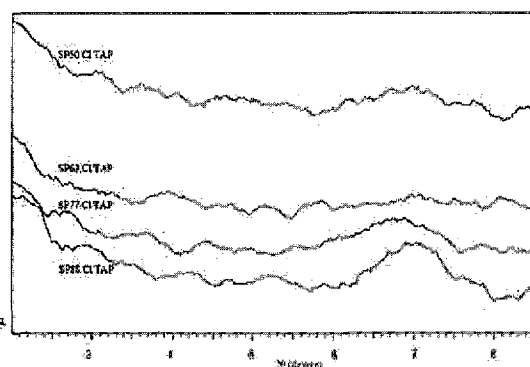


Figure 5 XRD patterns of SPEEK nanocomposite membranes as a function of degree of sulfonation (DS)

because the dispersion state of the clay particles can simply be obtained by analyzing the (001) lattice spacing of the clay [21]. The analysis of the commercial Cloisite15A<sup>®</sup> reveals the presence of two peaks at  $2\theta = 2.6^\circ$  and  $2\theta = 7.1^\circ$ . The corresponding lattices spacing of these planes are 3.4 nm and 1.24 nm, respectively. The first peak indicates the incorporation of the functional salt molecules into the Cloisite15A<sup>®</sup> clay structure. However, all SPEEK/ Cloisite15A<sup>®</sup> /TAP membranes showed featureless of this diffraction peak in which indicates a successful incorporation of Cloisite15A<sup>®</sup> in SPEEK matrices [14]. The second diffraction peak performed the position of plane (001) of Cloisite15A<sup>®</sup> clay [21]. From Figure 5, it can be seen that all SPEEK nanocomposite membranes showed lower intensity of the plane (001) diffraction peak than that of pure Cloisite15A<sup>®</sup>. Therefore, it can be deduced that the Cloisite15A<sup>®</sup> particles were successfully integrated in the SPEEK polymer matrix because of the presence of TAP. Excluding SP63/CL/TAP membrane, it was observed that, the intensity of the peak that corresponding to the plane (001) increased as the DS of the SPEEK nanocomposite membranes increased. The high intensity of the corresponding peak for the SP77/CL/TAP and SP88/CL/TAP membranes occurred might be because of the cracks observed on the surface of the membranes as confirmed by the FESEM images. SP77/CL/TAP and SP88/CL/TAP membranes showed the diffraction peak at

$2\theta = 6.9^\circ$  ( $d_{001} = 1.28$  nm) and  $7.05^\circ$  ( $d_{001} = 1.25$  nm), respectively. Since that both particular composite membranes showed higher  $d_{001}$  than the pure Cloisite15A<sup>®</sup>, it means that the intercalated nanocomposite is obtained. The broadening peak of the diffraction plane (001) for the SP50/CL/TAP membrane indicates a possible formation of partial exfoliation composite structure. The failure of SP50/CL/TAP membrane to perform exfoliation composite structure might be due to the low concentration of sulfonic acid group in the polymer matrix that that can be attached to the Cloisite15A<sup>®</sup>. Interestingly, it can be seen that, SP63/CL/TAP sample shows the broadest of the peak at plane (001) until the peak seems cannot be observed. This finding indicates that a partial exfoliated or exfoliated nanocomposite structure has been formed [22]. It can be concluded that the addition of Cloisite15A<sup>®</sup> particles in the appropriated or optimum degree of sulfonation (DS) of SPEEK, i.e., 63 %, along with the TAP assistance provides the best compatibility that possibly served a better polymer-inorganic nanocomposite electrolytes for DMFC application.

### 3.5 Swelling Behavior Study

The solubility properties, uptake behavior and dimensional stability of membranes are important parameters to take into consideration for the performance of DMFC. In this study, water and

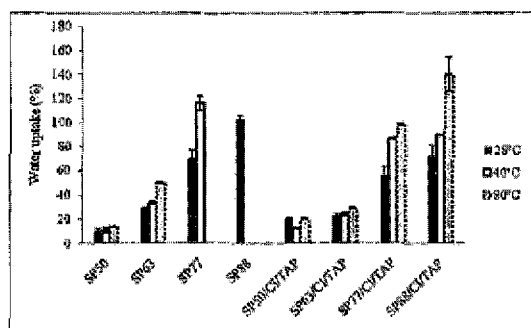
methanol uptake and dimensional stability of the membranes were chosen as the parameters to express the swelling behavior of the membrane. In fact in membranes made of sulfonated aromatic polymers, such as SPEEK, excessive swelling may lead to mechanical degradation and poor dimensional stability [23]. Therefore, it is crucial to further study the membrane stability in water and methanol solutions at room temperature or even at higher temperature for long term durability in the real DMFC system.

Figure 6 illustrates the water uptake of SPEEK and SPEEK nanocomposite membranes for different DSs and temperatures. As can be seen, the water uptake of SPEEK increased with increasing DS and temperature. A similar trend was observed for SPEEK nanocomposite membranes. However, SPEEK nanocomposite membranes exhibited lower water uptake than their parent SPEEK membranes of the similar DS, except for the SP50/CL/TAP membrane. Higher absorption capacity of SP50/CL/TAP than its parent SPEEK seems more natural considering the enhancement in the polarity in the composite membrane [24]. Surprisingly, other SPEEK nanocomposite membranes showed relatively lower water uptake as compared to their parent SPEEK membranes. It might suggest that a more compact network structure was formed, mainly due to (i) hydrogen bonding between amine groups ( $\text{NH}_2$ ) of TAP and sulfonic acid, ether and/or ketone groups of SPEEK and carbonyl groups of Cloisite15A<sup>®</sup>, and/or (ii) electrostatic interaction between quaternary ammonium ion

( $-\text{NH}_4^+$ ) of Cloisite15A<sup>®</sup> and sulfonic acid groups. This interaction behavior has restricted sulfonic acid ( $\text{SO}_3\text{H}$ ) groups and other polar groups from playing their roles in absorbing excessive water [25]. However, the reduction in water absorption of SPEEK nanocomposite membranes observed was not too strong. In other words, the moderate and appropriate water retained in SPEEK nanocomposite membranes was still encouraging other properties especially the conductivity.

The solubility properties of SPEEK nanocomposite membranes were much improved compared to the parent SPEEK membranes. For example, the SP88 membrane starts to dissolve in water at 40°C and SPP77 membrane is soluble at 80°C. On the other hand, both SP88/CL/TAP and SP77/CL/TAP membranes were insoluble in water even at 80°C. It is suggested that the solubility of SPEEK nanocomposite membrane was dominantly dependent on the barrier properties towards highly polar molecules such as water that are possessed by the inorganic filler such as Cloisite15A<sup>®</sup> [9].

The methanol uptake capability that is related to the electrochemical properties of the polymer electrolyte membranes was also determined. Figure 7 presents the water and methanol uptakes of SPEEK and SPEEK nanocomposite membranes with various DSs at room temperature. The amount of water and methanol uptakes in the SPEEK membranes were strongly dependent upon the amount of sulfonic acid groups attached. Similar trend was observed for SPEEK nanocomposite membranes. Interestingly, all SPEEK and SPEEK nanocomposite membranes except SP88 showed lower methanol uptake than that of water uptake. It was agreed that degree of swelling of polymeric membrane in solvent is proportional to the hydrogen bonding capability of solvent. The hydrogen bonding in methanol is not as strong as it is in water. This is because the O atom (from water or methanol molecules) does not have as much as partial negative charge in methanol as it does in water since the C (from methanol molecule) atom draws away some of the negative charge and simultaneously makes the hydrogen atom in methanol does not have as much positive charge as in water. Hence, it can be concluded that the



**Figure 6** Water uptake of SPEEK and SPEEK nanocomposite membranes for different DSs and temperatures

higher uptake in water was caused by high formation of hydrogen bonding formed in which enhanced the facilitation of water absorption into the membrane [26-27].

Figure 7 also shows that SPEEK and its nanocomposite membranes, except SP88, showed a gradual decreased methanol uptake while increasing methanol concentration up to 2 M. A comparable finding was reported by Yang on SPEEK/polyvinyl alcohol (PVA) blends membranes [28]. Interestingly, SP63, SP50/CL/TAP and SP63/CL/TAP membranes showed a remarkable influence on the absorption behaviors in methanol solution with concentration of 3 M and 5 M, whereas SP77 and SP88 and their nanocomposites with similar DS were degradable. As discussed above, this probably due to the reactivity changes of hydrogen bonding in methanol in which assist to an increase in the polarity of the methanol as in total when the methanol solution concentrations increased [26]. In addition, it was also suggested that the higher concentration of methanol solutions used results in higher methanol uptake was caused by the potentially higher rates of methanol transport into the membranes [29].

It clearly shows that Cloisite 15A<sup>®</sup> and TAP loadings has significant effects on the swelling behavior in methanol solutions. The addition of Cloisite 15A<sup>®</sup> and TAP decreased the methanol uptake at all tested methanol concentrations. In other words, Cloisite 15A<sup>®</sup> and TAP limit the

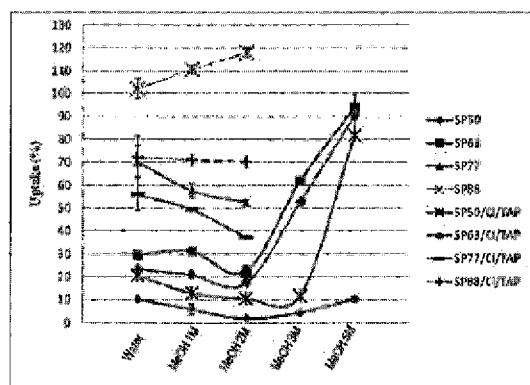


**Figure 7** Water and methanol uptakes of SPEEK and SPEEK nanocomposite membrane with various DSs as a function of methanol concentration

solvent uptake activities in SPEEK nanocomposite membranes to avoid an excessive swelling. Besides having the advantages of high aspect ratios of Cloisite 15A<sup>®</sup>, the lower solvent uptake of SPEEK nanocomposite membranes as compared to SPEEK membranes for both in water and methanol is also suggested contributed by the presence of TAP since the O atoms (from sulfonic groups and functional groups of Cloisite15A<sup>®</sup>) are already bound to TAP and the amount of available O atoms to produce hydrogen bonding with water and methanol become less, thus reducing the water and methanol uptakes in SPEEK nanocomposite membranes [14, 26]. This behavior also suggests a lower mass diffusion transfer through the SPEEK nanocomposite especially SP63/CL/TAP as compared to SP63 in the range of methanol concentrations tested. This evidence is confirmed by open circuit voltage (OCV) values obtained from polarization measurements (Figure 10).

Table 2 shows the dimensional changes resulting from immersion of the membrane in water and methanol solution (1 M) for the SPEEK and SPEEK nanocomposite membranes. The introduction of Cloisite15A<sup>®</sup> and TAP significantly contributed to a positive impact on the swelling behavior of SPEEK membranes. It can be seen that, the addition of Cloisite15A<sup>®</sup> and TAP decreased the swelling ratio in plane direction and increased that in thickness direction from parent SPEEK membranes to nanocomposite SPEEK membranes for both water and methanol solution. Interestingly, some SPEEK nanocomposite membranes such as SP88/CL/TAP showed the negative sign for the swelling in plane value (membrane diameter became shorter after soaking in 1M methanol solution) due to the significant increase in its thickness direction. This significant finding gives a beneficial impact to the real DMFC system as this behavior might reinforce the contact between current collectors and membrane electrolyte assembly (MEA), thus increase the overall DMFC performance [28, 30].

The remarkable improvement in the swelling properties observed for the SPEEK nanocomposite membranes, especially for the SP88/CL/TAP membrane encourages us to use

**Table 2** Swelling properties of SPEEK and its nanocomposite membranes in water and methanol (1 M)

Sample	Water		Methanol (1)			
	Thickness (mm)	Swelling in plane (%)	Swelling in thickness (%)	Thickness (mm)	Swelling in plane (%)	Swelling in thickness (%)
SP50	0.052±0.002	0	7.77±0.11	0.05±0.001	2±2.83	12±0.10
SP63	0.029±0.003	0.4±0.30	12.25±2.18	0.056±0.001	3±2.03	19.62±1.41
SP77	0.058±0.001	7.1±0.41	31.90±1.22	0.046±0.001	29±0.57	31.51±1.41
Sp88	0.077±0.002	8.0±1.00	-10.01±0.4	0.026±0.003	62±18.02	11.61±3.49
SP50/CL/TAP	0.043±0.001	0	10.47±1.65	0.049±0.002	2±1.32	3.07±2.83
SP63/CL/TAP	0.047±0.001	0	19.16±0.58	0.041±0.001	4±2.35	18.34±2.83
SP77/CL/TAP	0.042±0.001	3.2±3.32	15.65±1.44	0.043±0.001	24±1.46	5.79±5.66
SP88/CL/TAP	0.035±0.001	5.8±4.96	71.43±0	0.049±0.002	-11.17±1.27	287.26±11.31

SPEEK of high DS for the fabrication of polymer electrolyte membranes for DMFC by incorporating Cloisite15A<sup>®</sup> and TAP.

### 3.6 Proton Conductivity of SPEEK and SPEEK Nanocomposite Membranes

Water content of polymeric material has a considerable effect on proton conductivity. The higher the water content, the higher the conductivity will be. However, for polymer-inorganic membrane materials, the proton conductivity is also strongly dependant on the type of functional groups present in the inorganic filler [9]. It is proven to be partially true when the water uptake values in Figure 6 are compared with the proton conductivity results depicted in Figure 8; i.e., the conductivity of the SPEEK membrane increases together with the water uptake as the DS increases until the conductivity finally reaches  $8.15 \times 10^{-3} \text{ S cm}^{-1}$  at 25°C for the SP88 membrane. In fact, the high ionic conductivity at the elevated sulfonation level is attributed to the more interconnection of swollen ionic domains of the membrane to form a well-connected network structure, which facilitates proton conduction [31].

The SPEEK nanocomposite membranes behave similarly. The proton conductivity increases together with the water uptake as the DS increases. It should be noted that the proton conductivities of the SP63/CL/TAP and SP77/CL/TAP nanocomposite membrane were  $1.02 \times 10^{-2} \text{ S cm}^{-1}$  and  $1.03 \times 10^{-2} \text{ S cm}^{-1}$ , respectively. These values are close to that of Nafion112 obtained under a similar condition, which is  $1.16 \times 10^{-2} \text{ S cm}^{-1}$ . In particular, the proton conductivity of the SP88/CL/TAP nanocomposite membrane was  $1.47 \times 10^{-2} \text{ S cm}^{-1}$ , which was higher than that of Nafion112. However, when the proton conductivity and the water uptake data of the SPEEK composite membranes are compared with those of the parent SPEEK membranes, a contrasting effect of the water uptake is observed, i.e. despite the decrease in water uptake, the proton conductivity remarkably increases from the SPEEK membrane to the SPEEK composite membrane.

Therefore, it is concluded that the proton conductivity of SPEEK nanocomposite membranes depends on the functional groups involved. The availability of a strong ionic group in Cloisite15A<sup>®</sup>, i.e., quaternary ammonium salts significantly increases the proton conductivity of

the parent SPEEK membrane. In other words, the high proton conductivity of the SPEEK nanocomposite membranes is not only contributed by the  $\text{SO}_3\text{H}$  group in the SPEEK matrix but also from the conductive group in Cloisite15A<sup>®</sup>. The proton conductivity of SPEEK nanocomposite membranes was further enhanced by the exfoliated composite structure. Particularly in the case of SP63/CL/TAP membrane, nanosized ionic clusters are formed and will be available for proton conduction and make protons more mobile [32, 21].

### 3.7 Methanol Permeability of SPEEK and SPEEK Nanocomposite Membranes

In general, incorporation of the silicate layers into polyelectrolytes restricts the accessible nanometric channels for migration of polar molecules such as hydrogen ions, water and methanol molecules. This approach is crucial because membranes with lower methanol permeability allow higher methanol feed concentration, thus promoting the effective energy density of a fuel cell system [33]. Figure 8 shows that methanol permeability values of the SPEEK membranes increase as the DS increases. A similar trend was observed for the SPEEK nanocomposite membranes. The increment in methanol permeability is closely related to the water uptake ability of the membranes. From Figure 8, a dramatic decrease in methanol permeability is observed from the SPEEK to the nanocomposite membranes of the same DS. A comparable finding was also reported by a number of researchers [34-36]. The shape of Cloisite15A<sup>®</sup> nanofiller has a longer length than its width. The ratio of length to width of the filler is known as the aspect ratio. High aspect ratios of Cloisite15A<sup>®</sup> particles effectively reduce the area available for the methanol diffusion process. The lamellar elements (stacked silicate layers) of Cloisite15A<sup>®</sup> not only display high aspect ratio but also high in-plane strength until Cloisite15A<sup>®</sup> was able to discriminate methanol molecules to pass through it [37]. This behavior has significantly contributed to the decrease of methanol permeability of the SPEEK nanocomposite membranes. Unfortunately, both

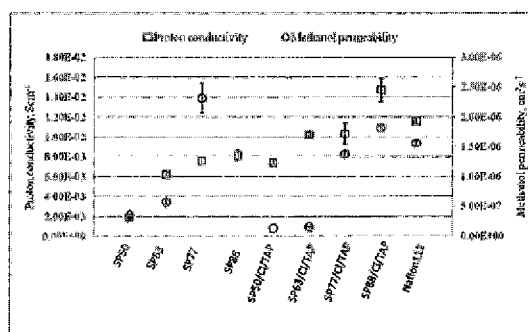


**Figure 8** Proton conductivity and methanol permeability of SPEEK and SPEEK nanocomposite membranes

SP77/CL/TAP and SP88/CL/TAP nanocomposite membranes showed increase in methanol permeability from SP50/CL/TAP and SP63/CL/TAP nanocomposite membranes. Probably, the defects on the surface of the SP77/CL/TAP and SP88/CL/TAP membranes, as observed in the FESEM images given in Figure 2(c) and (d), caused those membranes to exhibit high methanol permeability. This is due to poor dispersion of Cloisite15A<sup>®</sup> fillers at the fractured areas on the membrane surface. Thus, the intrinsic methanol permeability of the parent SPEEK was quickly approached.

### 3.8 Membrane Selectivity

Addition of Cloisite15A<sup>®</sup> and TAP to SPEEK has an important influence on both the proton conductivity and methanol permeability. In order to identify the optimum membrane from the tested membranes, it is worth analyzing the membrane dependency on the ratio of the protonic conductivity to the methanol permeability (membrane selectivity). From Figure 9, a significant fluctuation in the membrane selectivity values is observed. For SPEEK membranes, the selectivity for SP63 is the highest. This was apparently due to a dramatic increase in proton conductivity from SP50 to SP63. For SPEEK nanocomposite membranes, the selectivity values for SP50/CL/TAP and SP63/CL/TAP are not significantly different, since the methanol permeabilities of these membranes are almost the same. However, SP63/CL/TAP membrane

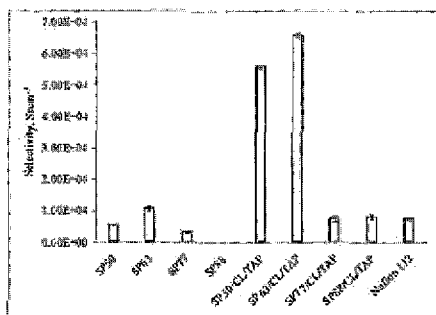


**Figure 9** Selectivity of SPEEK and SPEEK nanocomposite membrane

showed a slightly higher selectivity due to its higher proton conductivity. Beyond 63% DS, the membrane selectivity decreases for both the SPEEK and the nanocomposite membrane mainly because of a dramatic increase in methanol permeability.

From these results it can be concluded that the SP50/CL/TAP and the SP63/CL/TAP membranes are the best among the studied membranes in terms of their selectivity.

### 3.9 DMFC Performance

Polarization measurements can also be used to verify the impact of conductivity and methanol permeability on MEA behavior. Figure 10 summarizes polarization curves of cell potential versus current density and power density versus current density obtained from SP63 and SP63/CL/TAP with 3 M methanol solution.

The open circuit voltage correlates with the crossover of methanol through the MEA. Since similar electrodes were used throughout the DMFC performance testing, it can be said that the OCV is reduced by mass diffusion [38]. OCV values in Figure 10 indicated that the higher is the mass diffusion (as previously discussed) the lower is the OCV value. This effect is more evident for SP63 membrane than for SP63/CL/TAP when the OCV value of SP63 (0.51 V) recorded was lower than that of SP63/CL/TAP (0.54 V).

It was observed that, in the first two regions of cell potential versus current density polarization curve, i.e., activation polarization and ohmic

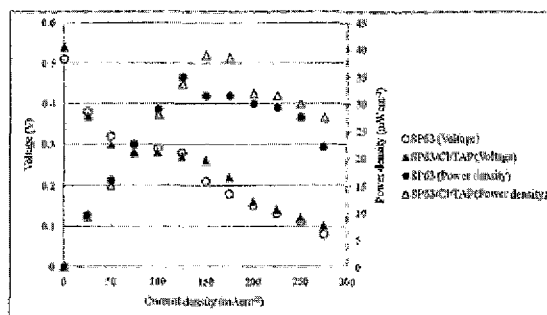


**Figure 10** Polarization curve of SP63 and SP63/CL/TAP MEAs

polarization, SP63/CL/TAP showed more voltage drop than that of SP63. Although SP63/CL/TAP exhibited higher proton conductivity value as shown in Figure 8, its ohmic polarization curve was more pronounced than SP63. This might be due to the increased of the interface resistance between electrodes and the membrane in the MEA attributed to the incompatibility of the MEA structure with the SP63/CL/TAP membrane [39]. Interestingly, it was discovered that SP63/CL/TAP shows wider ohmic polarization range of 75-175  $\text{mAcm}^{-2}$  as compared to SP63, i.e., 75-125  $\text{mAcm}^{-2}$ . In addition, the polarization curve was found to be affected by the mass transport limitation at 200  $\text{mWcm}^{-2}$  and 150  $\text{mWcm}^{-2}$  for SP63/CL/TAP and SP63, respectively. Hence, it was also observed that SP63/CL/TAP curve also showed lower voltage drop as compared to SP63 as a result of lower methanol crossover. Consequently this result indicated that the mass loss transfer is rather slow for the SP63/CL/TAP nanocomposite MEA. The highest power density recorded from SP63 and SP63/CL/TAP MEAs are 38.5  $\text{mWcm}^{-2}$  and 35  $\text{mWcm}^{-2}$ , respectively. The performance results indicated that the addition of Cloisite15A<sup>®</sup> and TAP have indeed enhanced the DMFC performances.

### 3.0 CONCLUSION

SPEEKs with various DSs were successfully mixed with Cloisite15A<sup>®</sup> in the presence of TAP as a compatibilizer. Considering its acceptable

proton conductivity, low methanol permeability and swelling stability, SP63/CL/TAP can be accepted as the optimum SPEEK nanocomposite membrane. It would be interesting to investigate the effect of Cloisite 15A<sup>®</sup> and TAP loading to optimize the membrane fabrication conditions. The incorporation of TAP allowed homogenous dispersion of filler particles in the matrix of SPEEKs with different DSs. The swelling stability was remarkably improved by the filler incorporation. In particular, SP88/CL/TAP membrane was found insoluble in water even at 80°C despite the very high DS of the SPEEK. The DMFC performance testing revealed that the SP63/CL/TAP nanocomposite membrane was outperformed SP63. Therefore, it can be concluded that the incorporation of both Cloisite 15A<sup>®</sup> and TAP is indeed an effective approach to improve the physicochemical properties and performance of SPEEK based electrolyte membranes for DMFC application.

#### ACKNOWLEDGEMENT

The authors are thankful to Universiti Teknologi Malaysia for the generous financial sponsorship to support one of the authors, i.e. Juhana Jaafar for her PhD study leave.

#### REFERENCES

- [1] Lobato, J., Cañizares, P., Rodrigo, M. A., Linares, J. J., Fernández-Fragua, A., 2006. Application of Sterion<sup>®</sup> Membrane as a Polymer Electrolyte for DMFCs. *Chemical Engineering Science*. 61: 4773-4782.
- [2] F. Dong, Z. Li, S. Wang, L. Xu, X. Yu, 2011. *Int. J. Hydrogen Energy*. 36: 3681-3687.
- [3] J. Lobato, P. Cañizares, M. A. Rodrigo, D. Úbeda, F. J. Pinar, 2011. *J. Membr. Sci.* 369: 105-111.
- [4] D. E. Moilanen, D. B. Spry, M. D. Fayer. 2008. *J. American Chem. Society*. 24(8): 3690-3698.
- [5] Yang, D., Li, J., Jiang, Z. Y., Lu, L., Chen, X., 2009. Chitosan / TiO<sub>2</sub> Nanocomposite pervaporation Membranes for Ethanol Dehydration. *Chemical Engineering Science*. 64: 3130-3137.
- [6] Carrado, K. A., 2000. Synthetic Organo- and Polymer-clays: Preparation, Characterization, and Materials Applications. *Applied Clay Science*. 17: 1-23.
- [7] Cervantes-Uc, J. M., Cauich-Rodriguez, J. V., Vazquez-Torres, H., Garfias-Mesias, L. F., Paul, D. R., 2007. Thermal Degradation of Commercially Available Organoclays Studied by TGA-FTIR. *Thermochimica Acta*. 457: 92-102.
- [8] Nagarale, R. K., Shin, W., Singh, P. K., 2010. Progress in Ionic Organic-inorganic Composite Membranes for Fuel Cell Applications. *Polymer Chemistry*. 1: 388-408.
- [9] Emmerich, K., Wolters, F., Kahr, G., Lagaly, G., 2009. Clay Profiling: The Classification of Montmorillonites. *Clays Clay Mineral*. 57: 104-114.
- [10] S. C. Chen, 2000. *Synthesis and Characterization of Polyurethane/clay Nanocomposite: Melt Compounding*. The University of Queensland, St. Lucia, Australia.
- [11] Othman, M. H. D., Ismail, A. F., Mustafa, A., 2007. Proton Conducting Composite Membrane from Sulfonated Poly (ether ether ketone) and Boron Orthophosphate for Direct Methanol Fuel Cell Application. *Journal of Membrane Science*. 299: 156-165.
- [12] Ismail, A. F., Othman, N. H., Mustafa, A., 2009. Sulfonated Polyether Ether Ketone Composite Membrane using Tungstosilicic Acid Supported on Silica-aluminium Oxide for Direct Methanol Fuel Cell (DMFC). *Journal of Membrane Science*. 329: 18-29.
- [13] Mohd Norddin, M. N. A., Ismail, A. F., Rana, D., Matsuura, T., Mustafa, A., Tabe-Mohammadi, S., 2008. Characterization and Performance of Proton Exchange Membranes for Direct Methanol Fuel Cell: Blending of Sulfonated Poly(ether ether ketone) with Charged Surface Modifying Macromolecule. *Journal of Membrane*

- Science*. 323: 404-413.
- [14] Jaafar, J., Ismail, A. F., Matsuura, T., 2009. Preparation and Barrier Properties of SPEEK/Cloisite 15A@TAP Nanocomposite Membrane for DMFC Application. *Journal of Membrane Science*. 345: 119-127.
- [15] Mohd Norddin, M. N. A., Ismail, A. F., Rana, D., Matsuura, T., Tabe, S., 2009. The Effect of Blending Sulfonated Poly(ether ether ketone) with Various Charged Surface Modifying Macromolecules on Proton Exchange Membrane Performance. *Journal of Membrane Science*. 328: 148-155.
- [16] Othman, M. H. D., Ismail, A. F., Mustafa, A., 2007. Physico-Chemical Study of Sulfonated Poly(Ether Ether Ketone) Membranes for Direct Methanol Fuel Cell Application. *Malaysian Polymer Journal*. 2: 10-28.
- [17] Nguyen, T. H., Wang, X., 2009. Fabrication of the Porous Polyimide Film as a Matrix of the Composite Membrane of the Direct Methanol Fuel Cell. *Separation and Purification Technology*. 67: 208-212.
- [18] Roelofs, K. S., Hirth, T., Schiestel, T., 2010. Sulfonated Poly(ether ether ketone)-based Silica Nanocomposite Membranes for Direct Ethanol Fuel Cells. *Journal of Membrane Science*. 346: 215-226.
- [19] Hasani-Sadrabadi, M. M., Dashtimoghadam, E., Majedi, F. S., Kabiri, K., 2009. Nafion@Bio-functionalized Montmorillonite Nanohybrids as Novel Polyelectrolyte Membranes for Direct Methanol Fuel Cells. *Journal of Power Sources*. 190: 318-321.
- [20] Kim, S., Hwang, E. J., Jung, Y., Han, M., Park, S., 2008. Ionic Conductivity of Polymeric Nanocomposite Electrolytes based on Poly(ethylene oxide) and Organo-clay Minerals. *Journal of Colloids Surface A*. 313-314: 216-219.
- [22] Villaluenga, J. P. G., Khayet, M., Lopez-Manchado, M. A., Valentin, J. L., Seoane, B., Mengual, J. I., 2007. Gas Transport Properties of Polypropylene/clay Composite Membranes. *European Polymer Journal*. 43: 1132-1143.
- [23] Frounchi, M., Dabbin, S., Salehpour, Z., Nofaresti, M., 2006. Gas Barrier Properties of PP/EPDM Blend Nanocomposite. *Journal of Membrane Science*. 282: 143-248.
- [24] Li, L., Zhang, J., Wang, Y., 2003. Sulfonated Poly(ether ether ketone) Membranes for Direct Methanol Fuel Cell. *Journal of Membrane Science*. 226: 159-167.
- [25] M. M. Hasani-Sadrabadi, E. Dashtimoghadam, S. R. Ghaffarian, M. H. Hasani Sadrabadi, M. Heidari, H. Moaddel, 2010. *Renewable Energy*. 35: 226-231.
- [26] Hasani-Sadrabadi, M. M., Dorri, N. M., Ghaffarian, S. R., Dashtimoghadam, E., Sarikhani, K., Majedi, F. S., 2010. Effects of Organically Modified Nanoclay on the Transport Properties and Electrochemical Performance of Acid-doped Polybenzimidazole Membranes. *Journal of Applied Polymer Science*. 117: 1227-1233.
- [27] Ismail, A. F., Zubir, N., Nasef, M. M., Dahlan, K. M., Hassan, A. R., 2005. Physicochemical Study of Sulfonated Polystyrene Pore-filled Electrolyte Membranes by Electrons Induced Grafting. *Journal Membrane Science*. 254: 189-196.
- [28] Godino, M. P., Barragán, V. M., Villaluenga, J. P. G., Izquierdo-Gil, M. A., Ruiz-Bauzá, C., Seoane, B., 2010. Liquid Transport through Sulfonated Cation-exchange Membranes for Different Water-alcohol Solutions. *Chemical Engineering Journal*. 162: 643-648.
- [29] Tao Yang, 2008. Preliminary Study of SPEEK/PVA Blend Membranes for DMF Applications. *International Journal of Hydrogen Energy*. 33: 6772-6779.
- [30] Heinzl, A., and Barragan, V. M., 1999. A Review of the State-of-the-art of the Methanol Crossover in Direct Methanol Fuel Cells. *Journal of Power Sources*. 84: 70-74.
- [31] Vona, M. L. D., Ahmed, Z., Serafina Bellitto, Alessandro Lenci, Enrico Traversa, Licoccia, S., 2007. SPEEK-TiO<sub>2</sub> Nanocomposite Hybrid Proton Conductive Membranes via in situ Mixed Sol-gel Process. *Journal of Membrane Science*. 296: 156-161.
- [32] Gao, Y., Robertson, G. P., Guiver, M. D., Jian, X., Mikhailenko, S. D., Wang, K., Kaliaguine, S., 2003. Sulfonation of Poly(phthalazinones) with Fuming Sulfuric Acid mixtures for Proton Exchange



- Membrane Materials. *Journal of Membrane Science*. 227: 39-50.
- [33] Wang M., and Dong, S., 2007. Enhanced Electrochemical Properties of Nanocomposite Polymer Electrolyte based on Copolymer with Exfoliated Clays. *Journal of Power Sources*. 170: 425-432.
- [34] Li, D., Chen, J., Zhai, M., Asano, M., Maekawa, Y., Oku, H., Yoshida, M., 2009. Hydrocarbon Proton-conductive Membranes Prepared by Radiation-grafting of Styrenesulfonate onto Aromatic Polyamide Films. *Nuclear Instrument Methods Physic Research Section B*. 267: 103-107.
- [35] Lin, Y. F., Yen, C. Y., Hung, C. H., Hsiao, Y. H., Ma. C. C. M., 2007. A Novel Composite Membranes based on Sulfonated MMT Modified Nafion for DMFC. *Journal of Power Source*. 168: 162-166.
- [36] Lin, Y. F., Yen, C. Y., Ma, C. C. M., Liao, S. H., Hung, C. H., Hsiao, Y. H., 2007. Preparation and Properties of High Performance Nanocomposite Proton Exchange Membrane for Fuel Cell. *Journal of Power Sources*. 165: 692-700.
- [37] Chuang, S. W., Hsu, S. L. C., Hsu, C. L., 2007. Synthesis and Properties of Fluorinecontaining Polybenzimidazole/montmorillonite Nanocomposite Membranes for Direct Methanol Fuel Cell Applications. *Journal of Power Sources*. 168: 172-177.
- [38] K. C. Chang, S. T. Chen, H. F. Lin, C. Y. Lin, H. H. Huang, J. M. Yeh, Y. H. Yu. 2008. *Europ Polym J.*, 44: 13-23.
- [39] Caracino, P., Ballabio, O., Colombo, M., Sala E., Cavallo, G., Faucitano, A., Buttafava, A., Dondi, D., 2009. Polymeric fluorine-free Electrolyte for Application in DMFC. *International Journal of Hydrogen Energy*. 34: 4653-4660.
- [40] Song, M-K., Park, S-B., Kim, Y-T., Kim, K-H., Min, S-K., Rhee, H-W., 2004. Characterization of Polymer-layered Silicate Nanocomposite Membranes for Direct Methanol Fuel Cells. *Electrochimica Acta* 50, 639-643. Nylon-6,6. *Polymer*. 33(2): 284-293.